MATERIALS SCIENCE

Moderated ionic bonding for water-free recyclable polyelectrolyte complex materials

Sophie G. M. van Lange[1]*, Diane W. te Brake[1], Giuseppe Portale[2], Anbazhagan Palanisamy[1], Joris Sprakel[3], Jasper van der Gucht[1]

While nature extensively uses electrostatic bonding between oppositely charged polymers to assemble and stabilize materials, harnessing these interactions in synthetic systems has been challenging. Synthetic materials cross-linked with a high density of ionic bonds, such as polyelectrolyte complexes, only function properly when their charge interactions are attenuated in the presence of ample amounts of water; dehydrating these materials creates such strong Coulombic bonding that they become brittle, non-thermoplastic, and virtually impossible to process. We present a strategy to intrinsically moderate the electrostatic bond strengths in apolar polymeric solids by the covalent grafting of attenuator spacers to the charge carrying moieties. This produces a class of polyelectrolyte materials that have a charge density of 100%, are processable and malleable without requiring water, are highly solvent- and water-resistant, and are fully recyclable. These materials, which we coin "compleximers," marry the properties of thermoplastics and thermosets using tailored ionic bonding alone.

INTRODUCTION

Ionic interactions between oppositely charged macro-ions can, when well controlled, form a versatile supramolecular strategy to assemble a wide diversity of materials. Nature has evolved complex biomolecular motifs that harness these electrostatic attractive forces to their fullest potential, ranging from strongly hydrated soft coacervates, such as membraneless organelles (*1*), to the dense packing of DNA in chromatin through complexation with histones (*2*), to tough and stiff nacre that relies on strong electrostatic bonding between proteins and mineral platelets (*3*, *4*). In the synthetic domain, soft complex coacervates (*5*) and moderately hydrated polyelectrolyte complex (PEC) materials (*6*), sometimes called saloplastics (*7*), have been studied extensively. In all of these examples, water is an essential plasticizer (*8*–*11*), together with salt ions that screen the polymeric charges (*12*). To go beyond nature and create materials that use ionic interactions as dynamic cross-linkers, but which do not require water as a plasticizer, the use of charge interactions turns out to be more challenging. PECs have been studied extensively, yet primarily in the hydrated state, and have failed to show useful properties when dehydrated, because the lack of an accessible glass transition below the degradation temperature makes these materials brittle and un-processable in the dry state (*12*). In ionomers, interactions between charged side groups on polymer chains and their counterions lead to toughness enhancement in thermoplastics, but only if the charge density is kept low to moderate (*13*). Increasing the charge density to more than, typically, 15 mol % of the monomers leads to the deterioration of the material properties, and increased water sensitivity (*14*, *15*). Because of these challenges, the full potential of charge interactions in water-free environments, for instance, as dynamic cross-links in plastics, has yet to be realized. Consequently, there are no strategies to date to create a thermoplastic that relies exclusively on charge interactions at a high density that is recyclable, processable, and malleable at elevated temperature, and which is insensitive to hydration levels. A crucial requirement to gain sufficient control over ionic interactions in the absence of water and salt is that the electrostatic forces must be tempered to achieve the plasticity that is needed for processing. We can take inspiration from the field of ionic liquids, where the addition of asymmetric bulky pendant groups tempers the electrostatic forces to lower their melting point and to frustrate crystallization (*16*). Macromolecules of ionic-liquid monomers, also known as poly-ionic liquids (*17*), have been studied in association with their small-molecule counterions, but not in PECs where all small-molecule ions are removed and no additional solvent is present (*18*).

In this work, we introduce a material concept, which we coin compleximers, which are thermoplastics with a 100% charge density, constructed exclusively from electrostatic interactions between oppositely charged polymers. The key principle is that of intrinsic plasticization in which we use extended hydrophobic tails on the charged monomers to moderate the electrostatic forces in the absence of water. Compleximers are ionically cross-linked materials that are moldable by hot-pressing, are recyclable, and, despite their high charge density, are insensitive to water and resistant to a range of organic solvents. Small-molecule ionic liquids can be added on demand to further tune the glass transition temperatures and material mechanics, serving the function of electrostatic plasticizers. Compleximers thus combine attributes from both thermoplastics and thermosets, the two most traditional polymer classes. As a result, they offer a distinctive ionic alternative to other thermally reconfigurable bonds such as associative dynamic covalent bonds in vitrimers (*19*).

RESULTS

Intrinsically screened polyelectrolytes form solid complexes in solution

PECs are formed when two polymers that bear oppositely charged side chains are combined in solution. The combination of a Coulombic attraction between the charged groups attached to the backbone and the gain in counterion entropy upon their release leads to the precipitation of a dense phase (*20*, *21*). This results in either very soft viscoelastic liquids, when hydration levels and ionic strengths are

[1]Physical Chemistry and Soft Matter, Wageningen University and Research, 6708 WE Wageningen, Netherlands. [2]Macromolecular Chemistry and New Polymeric Materials, Zernike Institute for Advanced Materials, University of Groningen, 9747 AG Groningen, Netherlands. [3]Laboratory of Biochemistry, Wageningen University and Research, 6708 WE Wageningen, Netherlands.
*Corresponding author. Email: sophie.vanlange@wur.nl

high (*22*), or very brittle solids, when water and counterions are completely removed (*23*). The concept of complexiers is to reduce the dependence on external plasticization by water and salt by introducing intrinsic (internal) plasticizers chemically attached to the polymers themselves. To this end, we took inspiration from ionic liquids and synthetized polyelectrolytes with bulky side chains attached to the charged moiety. The polycation is based on vinylbenzylchoride, quaternized post-polymerization with varying side chains, and the polyanion is based on styrenesulfonyl imides, with fluorinated side chains of two different lengths. By varying the side-group dimensions, we constructed pairs of oppositely charged polyelectrolytes whose ionic interactions vary gradually from strong [non-screened (NS)], to moderate [half-screened (HS)], to weak [screened (S)] (Fig. 1, A to C). The role of the hydrophobic tethers is to increase charge separation distances, moderating interaction strengths not only to promote malleability at elevated temperature but also to introduce hydrophobicity to reduce the water sensitivity that is prominent and problematic in ionic materials.

To form complexiers, the two individual polymers are first dissolved in a common (organic) solvent and brought into contact in a 1:1 charge stoichiometry to allow complex formation under vigorous mixing (schematic, Fig. 1D). This leads to the formation of a precipitate, which is the complexier in the presence of the counterion salt as a contaminant. This salt is removed by washing a number of times with MilliQ water until the ionic conductivity of the supernatant approaches that of pure water (fig. S1A). We verified that this effectively removes most small ions by wide-angle x-ray diffraction (WAXD) in which the characteristic peaks of salt crystals disappeared after washing (fig. S1, B and C). Subsequent drying of the complexiers yields solid powders, free from small-molecule ions, solvents, and water (Supplementary Text 1). We confirm that the complexes are approximately stoichiometric by x-ray photoelectron spectroscopy (XPS) analysis (fig. S2).

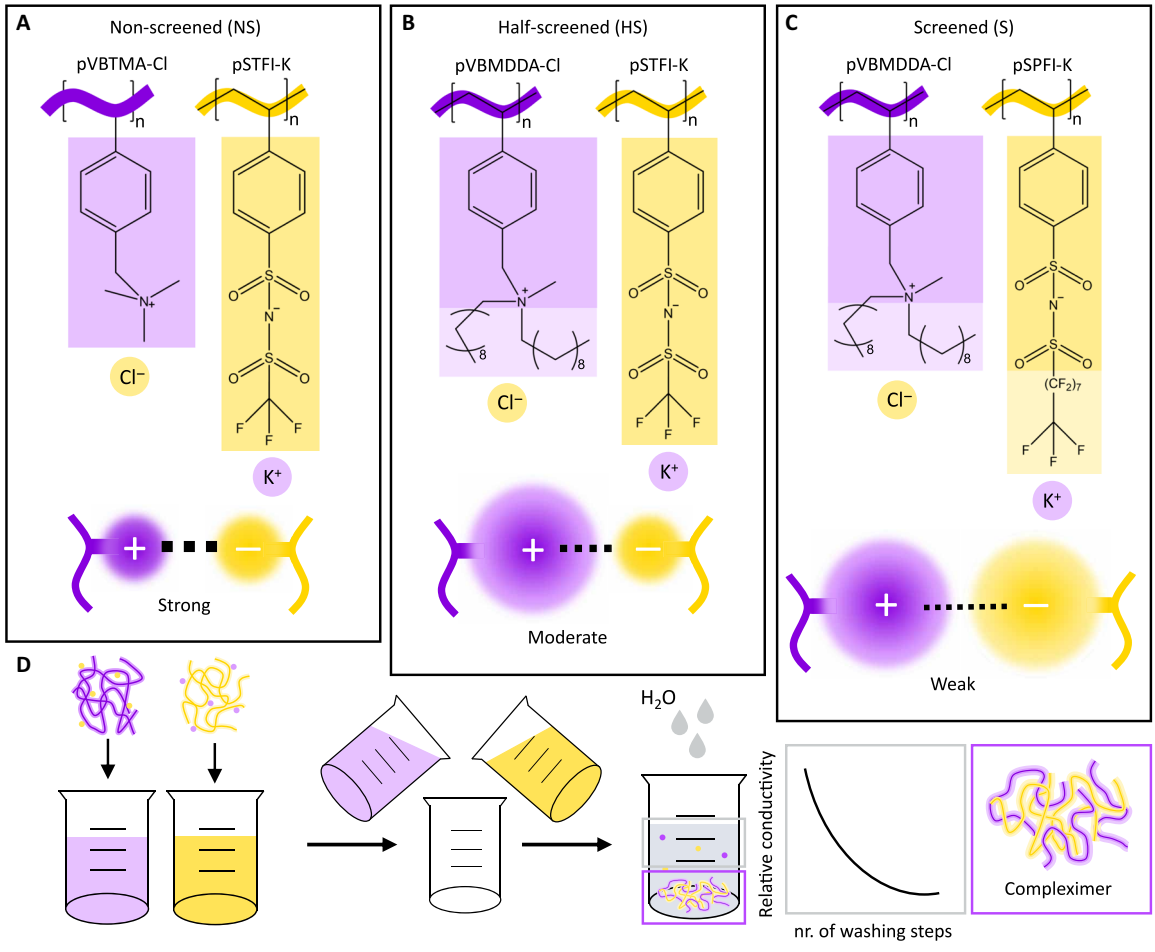

Fig. 1. Polyelectrolytes with varying degrees of intrinsic screening form complexiers upon mixing in solution. Four investigated polyelectrolytes consist of a polystyrene backbone with ionic liquid-inspired side chains. The alkyl and fluoroalkyl tail lengths are varied to modify the interaction strength. (**A**) Non-screened (NS) complexier has relatively accessible ionic groups, allowing for strong ionic bonding, similar to traditional PECs. (**B**) Half-screened (HS) complexier is made with a highly screened polycation, decreasing the strength of the ionic interactions in the complex. (**C**) Screened (S) complexier contains screening tails in both the polycation and the polyanion, leading to the weakest binding capability. (**D**) Schematic illustration of complexation. Complexiers are produced by dissolution of a respective polycation or polyanion and subsequent simultaneous mixing, which leads to the precipitation of a solid complex. These are washed with water until the conductivity reaches equilibrium close to the conductivity of MilliQ water, removing all free counterions from the complex. The final complexier is obtained as a dry powder. nr., number.

Screening of polyelectrolytes enables water-free processing and recycling

In traditional PECs, the removal of plasticizers causes the ionic bonding to become so strong that the glass transition temperature shifts up, often above their decomposition temperature, making processing impossible (*11*, *24*–*27*). Processability of these materials thus always requires the presence of both salt and water, hence the name saloplastics (*28*). Hydrophobic grafting of polyelectrolytes is known to affect the salt stability in PECs, usually increasing their salt resistance in solution (*29*–*32*). However, their mechanical properties remain largely determined by their hydration level, and the effect of hydrophobic screening of charged domains on mechanical properties in the absence of water has remained elusive.

We show that hot-pressing of our dry NS complexer, which is a weakly screened version of a traditional saloplastic material due to the ionic-liquid inspired side-chain chemistry, proves unsuccessful as the compressed material fails to fuse and remains heterogeneous and granular, even at temperatures up to 300°C (Fig. 2A). This evidences that the relatively weakly binding ionic-liquid moieties alone plasticize the material insufficiently. By contrast, increasing the level of charge screening further has a tremendous effect: the HS and S complexers are easily transformed into cohesive samples by hot-pressing. This validates our approach of intrinsic plasticization by side-chain attachment. We systematically varied the pressure and temperature to find the minimal temperature required for successful hot-pressing. The moderately screened HS complexer could be molded at a minimum temperature of 180°C, while increasing the level of screening in the S complexer reduced the processing temperature to 120°C.

Ionic interactions are dynamic and reversible in nature, so, unlike chemically cross-linked plastics, our electrostatically cross-linked complexers have the potential to be repeatedly reshaped and recycled. Processing of plastics at elevated temperatures may lead to material degradation, giving rise to performance loss during recycling (*33*). We investigate the thermal stability of our materials with thermogravimetric analysis (TGA) and find that the thermal stability of the individual polyelectrolytes is enhanced by complexation (Fig. 2B and fig. S3). We then performed isothermal TGA measurements at temperatures that correspond to the processing condition of HS complexer and S complexer (fig. S4) and find that the heat treatment of HS complexer during processing may lead to approximately 2% degradation. The processing of S complexer, however, occurs well below its degradation temperature (Fig. 2B and figs. S3 and S4).

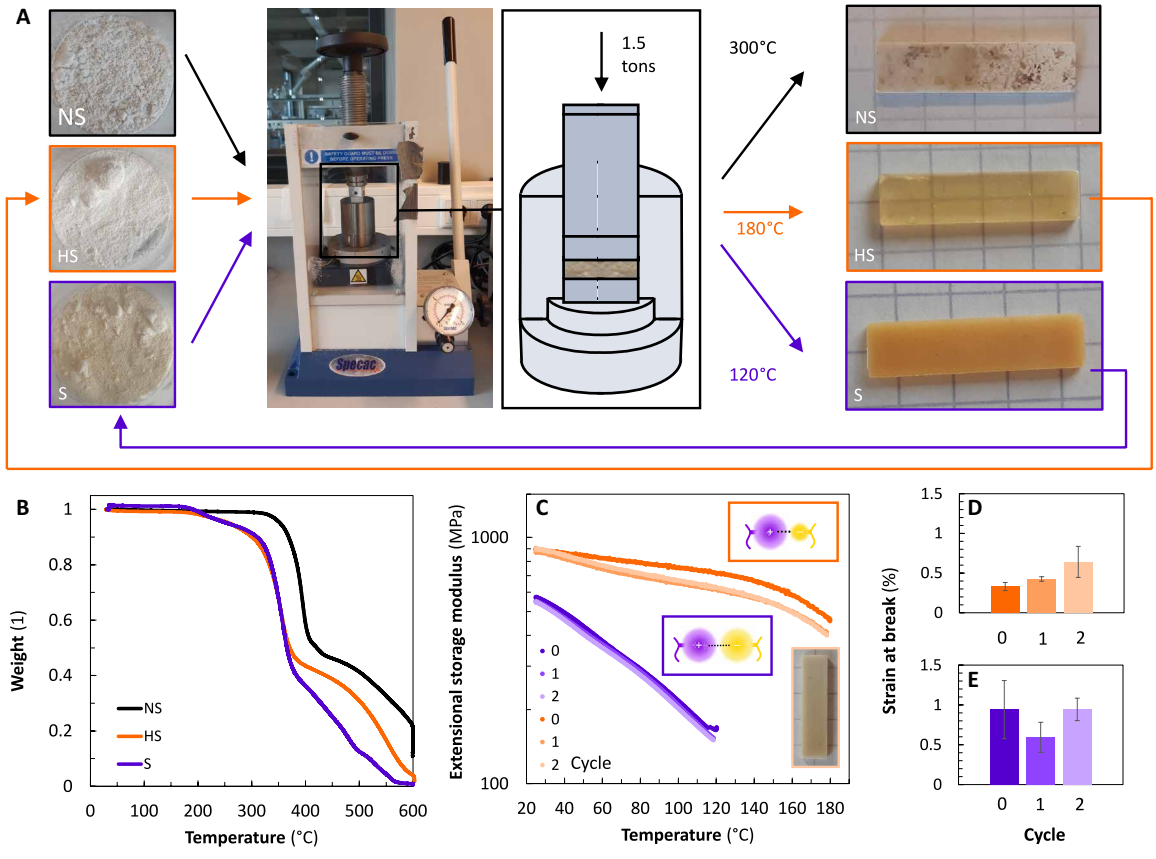

Fig. 2. Moderation of ionic interactions in complexers allows for successful processing and recycling without plasticizing solvents. (**A**) Ground, dry, complexer powder is hot-pressed, resulting in cohesive samples in case of moderate (HS) to weak (S) binding of the ionic moieties. NS complexer remains granular after processing under the proposed conditions, even at high temperatures. (**B**) TGA analysis of complexers reveals that strongly binding (NS) complexers have the highest thermal stability, followed by similarly degrading HS and S complexers. Processing occurs well below the respective degradation temperatures. (**C**) HS complexer (orange) undergoes an irreversible change in appearance and mechanical behavior upon recycling, transforming from transparent to turbid (see photo inset) with a lower modulus. The appearance and performance of S complexer (purple) is unaffected by recycling. (**D** and **E**) Mechanical performance of (D) HS complexer and (E) S complexer show that HS complexer weakens upon recycling, while S complexer recovers its original performance.

We monitor the evolution of the mechanical performance of HS and S complexiers up to their respective processing temperatures during multiple recycling steps. Recycling consists of grinding the formerly hot-pressed samples back to a powder and repeating the compression process. During the first reprocessing cycle of HS complexier, the material visually changes from a transparent to a turbid material, accompanied by a slight decrease in the extensional storage modulus (E') as measured by dynamic mechanical analysis (DMA) (Fig. 2C, orange, and inset). The change in mechanical properties is further confirmed by tensile testing, where we observe that the maximum extensibility increases upon recycling (Fig. 2D). The changes in turbidity emerge from the formation of voids, which we confirmed by scanning electron microscopy (SEM) (fig. S5, A and B).

It is plausible that chain scission occurs simultaneously with the degradation that was found with isothermal TGA or even before any observable weight loss. The repeated hot-pressing may thus lead to the presence of cleaved chains that can plasticize the material, explaining the affected mechanical properties of HS complexier. We conclude that HS complexier cannot be (re)processed below its degradation temperature without performance loss and therefore is not fully recyclable.

By contrast, repeatedly hot-pressing S complexier affects neither the extensional storage modulus (Fig. 2C, purple) nor the already turbid appearance resulting from some slight porosity (fig. S5C) and micro-phase separation (Supplementary Text 2). No performance is lost during recycling, as the mechanical properties recover fully (Fig. 2E), indicating the absence of notable chain scission events or degradation. This demonstrates that sufficient intrinsic screening of the charged domains of the polyelectrolyte pair allows for the formation of complexes that are malleable and recyclable without the need for any additional external plasticization. We further note that the mechanical properties of the complexiers remain stable upon storing the samples at ambient conditions for several months, without any signs of degradation or physical aging.

Ionic liquids are effective plasticizers of complexiers

The malleability of complexiers at elevated temperature suggests the presence of a thermal transition from a stiff to a soft material. Although thermal transitions have been observed in hydrated PECs (*10*, *11*), glass to rubber transitions are not known in dehydrated PECs below their thermal degradation point, owing to the extremely strongly interacting charges. The relatively weakly interacting ionic bonds in S complexier allow the material to soften with increasing temperature, shown by a gradual decrease of the extensional storage modulus. However, in its pure and pristine form, S complexier does not reach a glass transition temperature (T_g), which we define here as a peak in the loss tangent tanδ (= loss modulus E''/storage modulus E') measured by DMA in oscillatory mode in a temperature ramp (Fig. 3C and inset). We only find an onset of a transition, marked by an increase in tanδ and find a similar feature for pristine HS complexier (fig. S6). We gain control over the thermal transitions and mechanics in S complexier by varying the amount of three added plasticizers: the neutral plasticizer dioctylphthalate (DOP), as well as two ionic liquids that resemble the chemistry of these complexiers: screened methyl-trioctylammonium bis(trifluoromethylsulfonyl)imide (IL-S) and non-screened ethyldimethylpropylammonium bis(trifluoromethylsulfonyl)imide (IL) (fig. S7). The plasticizers are blended into the complexier powder with a ball mill. Plasticization with moderate amounts of neutral DOP (fig. S8) leads to the lowering of the storage modulus and gradually shifts the thermal transition to lower temperatures, suggesting that free alkyl chains plasticize the material to some extent. However, phase separation occurs at high concentrations of DOP, causing substantial deterioration of the material properties, which indicates the incompatibility of this uncharged additive with the charged complexier. This phase separation leads to a sudden loss in extensibility of the complexier, while still no glass transition is observed at elevated temperature.

By contrast, hot-pressing ionic liquid-plasticized complexiers leads to increasingly transparent samples with increasing concentrations for both IL-S (Fig. 3A) and IL (fig. S9A), which we attribute to the disappearance of macroscopic pores (fig. S5, C and D). Addition of increasing levels of ionic plasticizers allows us to systematically lower the T_g in complexiers and to modify the mechanics, supporting our hypothesis that the weakening of the ionic interactions is crucial for modifying the complexier's mechanical properties. Plasticization with IL-S, a highly screened and viscous ionic liquid decreases the modulus of the complexier moderately while strongly shifting the loss tangent curves to lower temperatures (Fig. 3 and fig. S10). We observe a glass transition, represented by a peak in tanδ, around 84°C in complexier plasticized with 20% IL-S (Fig. 3C and inset). Plasticization with a more liquid-like and less-screened ionic liquid, IL, has a stronger effect on lowering the modulus of the material (figs. S9B and S10) but decreases the glass transition temperature more moderately: a T_g of 140°C is found with 35% IL (fig. S9C and inset).

We find with small-angle x-ray scattering (SAXS) that ionic liquids at low concentration (5%) are absorbed by the complexier pores and do not lead to any detectable change of the network structure (Fig. 3D and fig. S9D). In samples with high concentrations (20% IL-S or 35% IL), structural differences occur that are represented by deviations from power law behavior of the SAXS profiles, which change slope for the 35% IL (fig. S9D) and change shape showing a broad intensity modulation for the 20% IL-S sample (Fig. 3D and Supplementary Text 2). Such features relate to conformational changes in the complexier microstructure, and, because the changes are more prominent upon plasticization with IL-S, this screened ionic liquid likely distributes more favorably in the complexier network due to its chemical likeness, possibly explaining its larger effect on the thermal properties. Using thermally resolved SAXS, which is sensitive to changes in the network density and in the network topology upon relaxation, (*34*) we observe that the microstructure of the pure complexiers does not change upon heating (fig. S11A). Focusing solely on the relative scattered intensity (Supplementary Text 3), which thus mainly represents the change in the material density, we find that pure complexier shows only a slight intensity decrease when heated from ambient temperature to 180°C (Fig. 3E). Conversely, the scattered intensity of complexier plasticized with 20% IL-S, upon heating, shows a rapid increase until 50°C, followed by a less marked increase at higher temperature. The transition temperature between these two regimes matches the onset of the tanδ curve quite closely. However, no notable changes in the SAXS curve of the 20% IL-S sample (i.e., no changes in the microstructure) are detected upon heating (fig. S11B). Changes in the scattered intensity of the complexier plasticized with 35% IL occur similarly at the onset of the tanδ modulation yet with very different effects. In this case, a marked drop of the SAXS intensity is observed starting at 80°C (fig. S9E) together with some minor changes in the shape of the SAXS curve (fig. S11C), associated with structural rearrangement of the system. Temperature-resolved SAXS thus reveals how the onset of the glass transition process in these plasticized complexiers is associated with

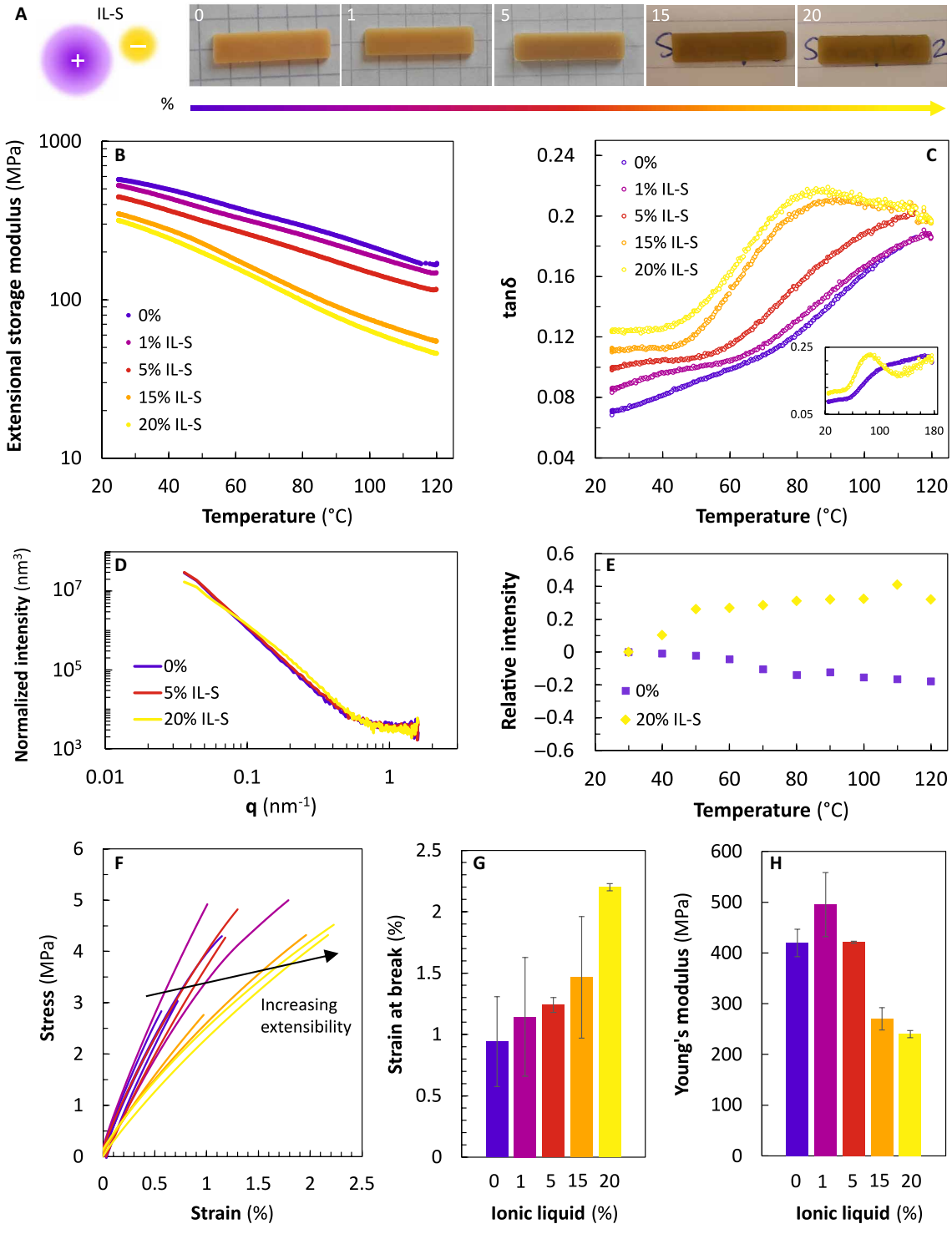

Fig. 3. Ionic screening as the key toward accessing glass transitions in complexiners. (**A**) A screened ionic liquid, methyl-trioctylammonium bis(trifluoromethylsulfonyl) imide (IL-S) is used to plasticize S complexiner by providing extrinsic screening. Samples become increasingly transparent with increasing plasticization. (**B**) The thermo-mechanical behavior of complexiner plasticized with increasing dose of ionic liquid confirms the successful plasticization observed as a decrease of the modulus. (**C**) The tanδ curve shifts to lower temperatures with increasing IL-S content, ultimately revealing glass transitions in the probed temperature range in samples plasticized with 15 to 20% of ionic liquid. The inset shows data on a broader *T*-range for the 0 and 20% IL-S samples. (**D**) Static SAXS reveals a change in the microstructure at 20% IL-S. (**E**) The relative intensity measured by temperature-resolved SAXS represents changes in the material density related to the thermal transition. (**F**) Tensile testing at room temperature shows an increasing trend in extensibility upon plasticization. This translates into (**G**) an increase in ultimate strain and (**H**) a decreasing trend in the magnitude of the Young's modulus.

changes in the material density for the 20% IL-S system and both changes in the material density and the network structure for the 35% IL system.

Glass transitions thus emerge in complexers upon further weakening of the ionic interaction strength by ionic liquid plasticization. Moreover, the maximal extensibility increases with increasing level of ionic liquid plasticization (Fig. 3, F to H, and fig. S8, F to H).

Complexers combine thermoplasticity with thermoset characteristics

Complexers are ionically cross-linked materials and show thermoplasticity when sufficiently plasticized with ionic liquids. Because the stiffness of plasticized complexers decreases gradually with increasing temperature, they can be easily reshaped under gentle heating with, e.g., a heat gun to deform the material into a spiral structure (Fig. 4A). Similarly, broken pieces can be quickly remolded in a hot-press at elevated temperature (Fig. 4B). Such manipulation of the shape of the material, especially in the absence of a sample mold, is comparable to the handling of silica glass and vitrimer materials (*35*).

In addition to the improved material handling and processing, complexers are insensitive to water. This distinguishes them from other ionic materials, in which the effect of water on the mechanical properties is notorious. Where 24 hours of immersion of a standard polyacrylic acid (PAA), poly(diallyldimethylammonium chloride) (PDADMAC) PEC in water results in considerable swelling and marked loss of mechanical properties over several orders of magnitude, the modulus of our complexer is hardly affected (Fig. 4C). The incorporation of bulky hydrophobic tails in polyelectrolytes thus not only improves the processability of complexers but also successfully generates sufficient hydrophobicity for water resistivity. Complexers are also insoluble in other (organic) solvents, similarly to thermosets. Immersion of S complexer in a variety of solvents shows the insolubility over a time span of 5 months (Fig. 4, D to M, and table S1). Complexers absorb trace amounts of water or salt solution (2.5 M KCl), in which PECs typically absorb a large fraction of their weight or dissolve completely. Immersion of the complexer in organic solvents such as dimethylformamide (DMF) and toluene causes swelling of the complexer. In IL-S, the complexer also shows no signs of dissolution. Complexers thus contain reconfigurable ionic interactions that give rise to solvent

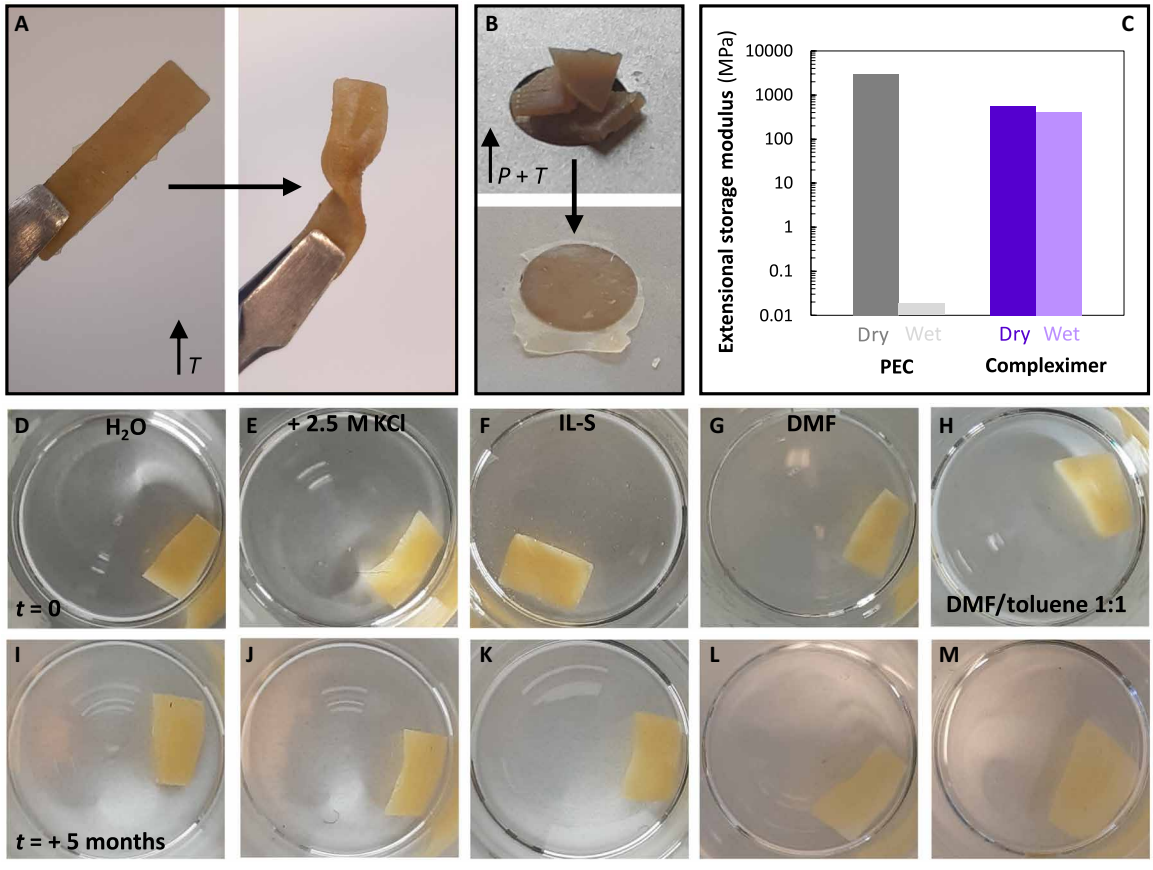

Fig. 4. Complexers are excellently malleable and solvent and moisture resistant. (**A**) A plasticized sample of S complexer (20% IL-S) can be deformed into a spiral shape upon heating with a heat gun. (**B**) Large pieces of plasticized S complexer (35% IL) can be easily molded into a new shape at elevated temperature. (**C**) Dried PEC of PAA-PDADMAC (dark grey) is extremely stiff but loses mechanical performance upon overnight immersion in water (light gray). The modulus of S complexer (dark purple) remains unaffected in water (light purple). (**D** to **M**) Samples of S complexer directly after immersion in a variety of solvents: (D) water, (E) 2.5 M KCl in water, (F) screened ionic liquid, (G) dimethylformamide (DMF), and (H) DMF/toluene 1:1. [(I) to (M)] Samples of S complexer immersed in said solvents for 5 months. No dissolution occurred, and samples swell in DMF and DMF/toluene.

resistance while also allowing for processing and recycling at elevated temperature.

DISCUSSION

The complexiomer materials presented in this work serve as a proof of concept for the use of moderated ionic bonding as a recyclable alternative to covalent cross-links in plastics. Complexiomers distinguish themselves from traditional PEC materials through the intrinsic screening of the ionic interactions by the attachment of bulky hydrophobic tails to the charged monomers. These hydrophobic polyelectrolytes form a complex when combined in solution, following the same driving force as traditional complex coacervation, but can be further used in the solvent-free state. When the hydrophobic tails attached to the charges are long enough, this leads to processable and recyclable materials that are resistant to water and other solvents. Our findings strongly suggest that weakening of the ionic interactions, by diluting the charged groups in the material and by sterically hindering their close proximity, is responsible for the improved processability. This is further confirmed by our observation that ionic plasticizers can very effectively lower the T_g and the elastic modulus of the materials. Nevertheless, the hydrophobic tails may also contribute to the processability in other ways, for example, by reducing friction between the backbones (Supplementary Text 4 and fig. S13). While it is difficult to distinguish between these two effects, we anticipate that a more detailed understanding of the precise role of ionic interactions in these materials can be obtained by systematic variation of the length of the attenuator groups and the density of charges along the backbone, together with quantitative measurements of the interaction strength between the polymers, for example, using single-molecule force spectroscopy (*36*), or by characterizing their phase behavior in solution (*37*).

The thermal transitions found in these complexiomers appear to be rather different from those commonly found in glassy polymers, where the extensional storage modulus decreases rapidly around the T_g and the peak in tanδ is much sharper. Complexiomers are relatively soft glasses that soften much more gradually over a broad range of temperatures. This behavior is reminiscent of vitrimers, of which the viscosity also gradually decreases with temperature, resulting from their characteristic intermolecular dynamics that follow the Arrhenius law. We cannot find a signature of the T_g with differential scanning calorimetry (DSC) (fig. S12), again suggesting that complexiomers may not have a sharp glass transition like traditional polymer glasses. It may well be that the long-ranged nature of the Coulomb interactions, as opposed to the short-ranged attraction of most other supramolecular bonds, blurs the notion of individual, localized bonds and leads to a very different type of thermal transition. A more detailed study of the relaxation dynamics in these materials at different temperatures and the role of the screened ionic interactions therein is required to obtain a better understanding of the nature of the thermomechanical transition.

Such systematic studies may also inspire further modification of the chemical structure to create improved polyelectrolyte combinations that do not need external plasticization to reveal thermal transitions or that produce materials with improved toughness. Achieving this probably requires not only changing the nature of the pendant chains but also exploring different polymer backbones with intrinsically lower T_g or lower charge densities. Moreover, to fully realize the sustainability of this material concept, we aim to investigate alternatives for the fluorinated side chains and their effect on the processability and water resistance.

In summary, we have demonstrated that carefully moderated ionic interactions can be used as a reversible alternative to covalent cross-linking in water-free PEC materials. We hope that the complexiomer concept will form an inspiration for exploring previously unidentified directions in the field of traditional PECs and to novel strategies for developing recyclable plastics.

MATERIALS AND METHODS

Materials

Sodium 4-vinylbenzenesulfonate (NaSSA; ≥90%), 4-vinylbenzyl chloride (VBC; 90%), *N*-methyldidecylamine (MDDA; 95%), 2,2′-azobis(2-methylpropionitrile) (AIBN; 98%), ammonium persulfate (APS; ≥98%), (vinylbenzyl)trimethylammonium chloride (VBTMAC; 99%), magnesium sulfate ($MgSO_4$; anhydrous), acetonitrile (ACN; anhydrous), DMF (anhydrous), ethyldimethylpropylammonium bis(trifluoromethylsulfonyl)imide (IL; 99%), methyl-trioctylammonium bis(trifluoromethylsulfonyl)imide (IL-S; >99%), DOP (>99.5), PAA solution (average M_w of ~250,000; 35 wt % in H_2O) and PDADMAC solution (average M_w of 200,000 to 350,000, 20 wt % in H_2O), and sodium hydroxide (NaOH; ≥98%) were purchased from Merck. Deuterated solvents were bought from Buchem. All other solvents were purchased form Biosolve. Oxalyl chloride [$(COCl)_2$; >98%], trifluoromethylsulfonamide (TFSA; >98%), and triethylamine (TEA; >99.0%) were obtained from TCI. Perfluorooctanesulfonamide (PFOSA; 97%) was received from SynQuest Laboratories. All chemicals were used without further purification.

Synthesis of pVBC

The synthetic procedure was adapted from a literature procedure (*38*). VBC (15.0 g, 99 mmol) was dissolved in 50 ml of toluene, followed by degassing with nitrogen for 10 min. AIBN (0.024 g, 0.15 mmol) was added, and the solution was degassed with nitrogen again. The reaction mixture was allowed to react for 16 hours at 60°C. The reaction mixture was allowed to cool down to room temperature, and the toluene mixture was concentrated before precipitation in cold methanol (300 ml). After filtration, the crude polymer was redissolved in 10 ml of chloroform and the precipitation was performed three more times. After the final filtration step, the polymer was dried in the vacuum oven overnight at 40°C and to obtain poly VBC (pVBC) as yellowish powder (4.44 g, 29.8%).

Synthesis of pVBMDDA-Cl

pVBC (3.0 g, 20 mmol) was dissolved in 50 ml of DMF (70°C, 30 min), and MDDA (12.3 g, 39 mmol) was added and allowed to react for 2 days at 70°C. The crude polymer mixture was precipitated in water (1 liter) and dried under vacuum overnight at 40°C to obtain a yellow solid (9.39 g, 61%).

Synthesis of pVBTMA-Cl

The synthesis protocol was modified from a published method (*39*). VBTMA-Cl (15,88 g, 75 mmol) was dissolved in 150 ml of demiwater and degassed with nitrogen for 30 min. After heating to 50°C, APS (34 mg, 0.15 mmol) was added, and the reaction mixture was allowed to react at 50°C for 20 hours. The viscous mixture was precipitated in 1 liter of cold tetrahydrofuran (THF) to obtain a white precipitation.

After filtration, the crude polymer mixture was dissolved in water and precipitated in THF again. Last, the THF was decanted, and the purified polymer was dried under vacuum for 20 hours (40°C) to obtain a white solid (14.57 g, 92%).

Synthesis of STFI-K

The synthetic method was based on reported methods in the literature, in which similar styrene-based polyelectrolytes were synthesized (*40*, *41*). Dry ACN (300 ml) was cooled to 0°C and degassed with N_2 for 40 min, before oxalyl chloride (13.58 g, 85.4 mmol) and anhydrous DMF (1 ml) were carefully added due to the strong exothermic reaction. The solution was stirred for 4 hours at room temperature to form the Vilsmeier-Haack complex. The solution was cooled down to 0°C, followed by the stepwise addition of NaSSA (16.0 g, 77.7 mmol) powder with backflow nitrogen, which results in the formation of NaCl precipitates. The mixture was stirred overnight at room temperature.

TFSA (11.57 g, 77.7 mmol) and TEA (19.61 g, 19.42 mmol) were dissolved in dry ACN and degassed for 30 min with a stream of nitrogen. The synthesis mixture with sulfonyl chloride solution was cooled down to 0°C, before the ACN solution with TFSA and TEA was slowly added. After reacting overnight [room temperature (RT), N_2], the mixture was filtered, and solvent was removed under vacuum. The resulting crude brown oily substance was dissolved in 50 ml of dichloromethane and extracted twice with a saturated sodium bicarbonate solution and once with brine, and the purified product was dried under vacuum. The obtained orange oil (6.73 g, 16.2 mmol) was mixed with a molar excess of K_2CO_3 (4.46 g, 32.3 mmol) solution in 80 ml of water and gradually changes to a yellow powder. After stirring for 2 hours, the mixture was centrifuged (15 min, 1500*g*) and redispersed in water, and this was repeated until the supernatant becomes colorless (about three to five times). Last, the supernatant was removed, and the product was dried in the vacuum oven at 30°C overnight, resulting in a white powder (4.52 g, 16%).

Synthesis of pSTFI-K

4-Styrenesulfonyl (trifluoromethylsulfonyl) imide (STFI) (4.52 g, 12.8 mmol) was dissolved in 30 ml of demiwater at 70°C and degassed with a stream of nitrogen for 20 min. APS (4.8 mg, 0.03 mmol) was added, and the mixture was degassed again for 10 min. The reaction mixture was stirred for 18 hours at 70°C. Water was evaporated, and the crude polymer was obtained as a sticky yellow sticky powder. This was dissolved in a few milliliters of dimethyl sulfoxide (DMSO) at elevated temperature (80°C, 30 min) and precipitated in 800 ml of cold THF. The precipitation solution was decanted, with a sticky polymer left in the beaker, and the procedure was repeated. After four precipitation steps, the polymer was dried under vacuum overnight at 40°C, and a yellow powder was obtained (4.31 g, 95%).

Synthesis of SPFI-K

The same experimental protocol as the potassium STFI (STFI-K) synthesis was used, with the only deviation that PFOSA (10.9 g, 24.3 mmol) was used instead of TFSA. A white powder was obtained (6.9 g, 40%).

Synthesis of pSPFI-K

A similar experimental protocol as for the poly STFI-K (pSTFI-K) polymerization was used, with the following deviations. 4-Styrenesulfonyl (perfluorooctanesulfonyl) imide (SPFI) (5.9 g, 8.3 mmol) and AIBN (4.8 mg, 0.029 mmol) were mixed in 50 ml of THF, which was purified by a small alumina column before. The reaction mixture was stirred for 18 hours at 70°C, and a glassy precipitation was formed over a few hours. After removal of THF, the crude polymer was dissolved in a few milliliters of DMSO and precipitated in cold water, lastly resulting in a white powder (4.04 g, 68%).

Nuclear magnetic resonance

^1H, ^{13}C, and ^{19}F nuclear magnetic resonance spectra were performed on a Bruker AV400 MHz spectrometer with $CDCl_3$, DMSO-d6, or D_2O as a solvent. Results are shown in table S2 and fig. S14.

Gel permeation chromatography

Gel permeation chromatography (GPC) measurements with organic solvents were performed using a Agilent Technologies 1200 system equipped with PLgel 5-µm, MIXED-D column and an Agilent 1200 RI detector thermostated using a Eppendorf CH-30 column heater with a TC-50 control unit. Samples were run at a flow rate of 1 ml/min using DMF with 0.1 wt % LiBr as eluent at 50°C or THF at 35°C. The calibration was performed using narrow molecular weight polystyrene standards.

GPC analysis with aqueous eluents were carried out at a Agilent Technologies 1200 infinity II with a Superdex 200 Increase 10/300 GL column and a Agilent 1260 RID detector. Analysis were performed with an aqueous solution containing 0.3 M $NaNO_3$ and 0.02 M NaH_2PO_4 as eluent at 35°C, a flow rate of 1 ml min^{-1}, and a calibration was carried out using polyethylene oxide standards. GPC results are shown in table S3.

Polyelectrolyte complexation

Polyelectrolytes were heated while stirring on an oil bath at 110°C in a 1:1 mixture of DMF/toluene at 0.055 M [to form HS from pSTFI-K and poly(vinylbenzyl methyldidecylammonium chloride) (pVBMDDA-Cl), and S complexiers from poly SPFI-K (pSPFI-K) and pVBMDDA-Cl] or water at RT [to form NS complexiers from pSTFI-K and poly(vinylbenzyl trimethylammonium chloride) (pVBTMA-Cl)] until fully dissolved (Supplementary Text 5). Equimolar amounts of the respective solutions of polycation and polyanion were mixed simultaneously and kept under stirred conditions (at 110°C or RT, respectively) overnight. The resulting suspensions were cooled down to room temperature and either centrifuged or precipitated in MilliQ water to isolate the solid precipitates. The supernatants were removed, and MilliQ water was added to wash out small counterions by vigorous stirring. The water was replaced twice per day for at least 3 days, which has been shown to effectively remove counterions (*42*). The resulting fine powders were filtered off and dried in a vacuum oven at 70°C for 3 days and then stored in a desiccator.

To create a reference PEC, PAA, and PDADMAC solutions were diluted to 0.125 M with MilliQ water, and the pH was adjusted to pH 7 with a NaOH solution, as described in the literature (*43*). The solutions were combined in equimolar amount, and the beakers were rinsed with some extra water. The solution was stirred overnight until the solution was fully transparent. The supernatant was decanted, and fresh MilliQ water was added and replaced every 12 hours for 3 days under stirring. Then, the MilliQ water was decanted and replaced by a 5:1 EtOH:H_2O solution for annealing, and this resulted in a more stiff complex suitable for processing.

Conductivity measurements

The supernatants obtained from each complexiner washing cycle were subjected to conductivity measurements using a Knick 703 conductometer equipped with a two-electrode probe with a cell constant of 1.08 cm^{-1}.

Hot-pressing

0.15 g of complexiner was added to a rectangular pressing die (20 mm by 5 mm, Zhengzhou TCH Instrument Co.). The die was preheated for 15 min at the desired temperature (NS, 300°C; HS, 180°C; and S, 120°C) in a Specac manual hydraulic press equipped with heated platens before a pressure of 1.5 tons was applied for (NS, 30 min; HS, 30 min; and S 15 min). After releasing the pressure, the sample mold was removed from the press and cooled down for at least 30 min before the sample was removed.

Soaked PAA-PDADMAC PEC was cut in pieces and patted dry with a paper towel. The material was transferred to a 30 mm–by–10 mm–by–1 mm flat sample mold and compressed at 80°C at 4 tons of pressure for 10 min between two smooth Teflon sheets. The sample plate was cooled inside the sample press and transferred to a desiccator with desiccant. When completely dry, the samples were removed from the mold and stored in a desiccator between two glass slides.

Ionic liquid plasticization

Pure S complexiner powder was added to a disposable 20 ml ball milling tube (IKA Laboratory Equipment). The percentage of plasticizer was based on the total polymer mass. The desired amount of ionic liquid, and 15 stainless steel balls were added to the tube. The powder was ground in three stages of 3 min with an IKA ULTRA-TURRAX Tube Drive at power level 9. Intermediately, the powder was scraped from the sides of the tube. Hot-pressing proceeded as described previously. At high levels of plasticization, 20% IL-S and 35% IL, the hot-pressed rectangular samples were broken in pieces and hot-pressed at 120°C for 5 min in a circular mold with a diameter of 7 mm and a thickness of 1 mm.

Recycling

Hot-pressed samples were pre-ground into a coarse powder with a Blaupunkt FCG701 coffee grinder. This coarse powder was then ground more finely in 20-ml IKA ball milling tube using the IKA ULTRA-TURRAX Tube Drive with 15 stainless steel balls at power level 9 in three cycles of 3 min with intermediate scraping. Hot-pressing followed as described previously.

Wide-angle x-ray diffraction

The WAXD studies were conducted using Bruker diffractometer in the reflection mode with the incident x-ray wavelength of 1.542 Å at a scan rate of 0.06° min^{-1}. Hot-pressed samples of 5 mm by 5 mm were used.

Scanning electron microscopy

SEM was performed on a FEI Magellan 400 (FEI Electron Optics B.V., The Netherlands) using an acceleration voltage of 2.0 kV. Complexiners were mounted on 90° aluminum stubs with double-sided adhesive, conductive carbon tape. Hot-pressed samples were broken in pieces. The fractured surface was oriented upward and sputter-coated with a 10-nm layer of tungsten (Leica EM SCD500, Leica Microsystems, The Netherlands).

Thermogravimetric analysis

A STA 6000 from Perkin Elmer was used to determine the thermal stability of the individual polymers and complexes. Approximately 5 mg of material was weighed and added to a ceramic sample cup. The samples were heated under an air flow of 20 ml min^{-1} at a rate of 10°C min^{-1} from 30° to 600°C and lastly kept isothermal for 5 min at 600°C.

Isothermal TGA measurements were performed by heating a sample from 30°C to the temperature of interest at a rate of 50°C min^{-1}. The sample was subsequently kept isothermal for a duration of 30 or 60 min, after which the temperature was increased at a rate of 20°C min^{-1} to study ascending temperatures. All measurements were done under an airflow of 20 ml min^{-1}.

Differential scanning calorimetry

We used a TA instruments DSC25 to measure the thermal response of complexiner samples, pure polymers, and plasticized complexiners. Approximately 7 mg of sample was weighed in an aluminum Tzero pan. We performed all measurements under a continuous nitrogen flow at 50.00 ml min^{-1} with an empty Tzero pan as reference. The samples were initially heated to 40°C and held isothermal for 5 min to equilibrate. Then, the temperature was increased to 200°C at a heating rate of 10°C min^{-1}, after which the temperature was held isothermal for 5 min again. The sample was subsequently cooled at the same rate, and the entire sequence was repeated to obtain data of two heating cycles. Before doing the DSC tests, different sample pans were heated in an oven of 200°C to ensure that the pans would remain closed in the machine.

X-ray photoelectron spectroscopy

A JPS-9200 photoelectron spectrometer (JEOL, Japan) was used to determine the elemental composition of the hot-pressed samples. The spectra were generated by applying monochromatic Al Kα x-ray radiation at 12 kV and 20 mA with an analyzer energy pass of 10 eV for narrow scans. Processing of the spectra was performed using the peak fitting program in CasaXPS software (version 2.3.24 PR1.0).

Dynamic mechanical analysis

An Anton Paar 702 Space Multidrive equipped with a DMA fixture was used for extensional oscillatory measurements. First, amplitude sweeps were performed at room temperature at 1 Hz to determine the linear viscoelastic regime of the materials. Then, a heating and subsequent cooling ramp (3°C min^{-1}) were performed between 25°C and the processing temperature (HS, 180°C; and S, 120°C) while oscillating with a strain of S of 0.1% and HS of 0.01% at a frequency of 1 Hz with a preload force of 1500 Pa. Two plasticized samples (20% IL-S and 35% IL) were additionally characterized in shear mode with a 7-mm plate-plate geometry using a preload force of 2 N at 1 Hz and an amplitude of 0.1%. The shear moduli were converted to extensional moduli by multiplying by 3.

Small-angle x-ray scattering

SAXS measurements were performed at the Multipurpose Instrument for Nanostructured Analysis in Groningen, The Netherlands. The instrument was equipped with a high flux Cu rotating anode (Bruker) and two-dimensional (2D) x-ray detectors. SAXS images were collected using a 2D Pilatus 300k (Dectris) detector placed 3 m away from the samples. Compression molded samples of 1 mm in thickness were placed inside a Linkam hot stage, allowing heating of the sample. Samples were contained in an aluminum pan equipped

with kapton windows. The temperature was increased stepwise every 10°C, and the samples were equilibrated for 10 min before each SAXS measurement. The beam center and the scattering angle scale were calibrated using the known position of diffraction rings from a Silver Behenate standard powder. After background subtraction, the 2D SAXS images were converted into the 1D SAXS intensity profiles using the FIT2D software [from European Synchrotron Radiation Facility (ESRF)], and the data were plotted against the modulus of the scattering vector $q = \frac{4\pi\sin\theta}{\lambda}$ where 2θ is the scattering angle and $\lambda = 0.15413$ nm is the x-ray wavelength.

Tensile testing

The rectangular samples were used for stress-strain experiments at least a the day after performing the temperature ramp. The samples were subjected to a linear stress ramp from 0 to 10 MPa at a speed of 0.5 MPa s^{-1} until they broke.

Solvent absorption

Samples were immersed in a variety of solvents and left in closed containers for several months. To quantify the absorption, these samples were patted dry with a paper towel and weighed. The samples were then dried under vacuum at 40°C. The samples were weighed after 1 and 2 days of drying. Because the dry weight was stable, the weight on the second day was used for further calculations. The mass percentage of absorbed solvent was calculated through $\frac{\text{Weight}_{\text{swollen}} - \text{Weight}_{\text{dry}}}{\text{Weight}_{\text{dry}}} * 100\,\%$.

Supplementary Materials

This PDF file includes:

Supplementary Texts 1 to 5
Figs. S1 to S14
Tables S1 to S3
References

REFERENCES AND NOTES

1. E. Gomes, J. Shorter, The molecular language of membraneless organelles. *J. Biol. Chem.* **294**, 7115–7127 (2019).
2. N. Korolev, O. V. Vorontsova, L. Nordenskiöld, Physicochemical analysis of electrostatic foundation for DNA–protein interactions in chromatin transformations. *Prog. Biophys. Mol. Biol.* **95**, 23–49 (2007).
3. N. Zhang, S. Yang, L. Xiong, Y. Hong, Y. Chen, Nanoscale toughening mechanism of nacre tablet. *J. Mech. Behav. Biomed. Mater.* **53**, 200–209 (2016).
4. N. Zhang, Y. Chen, Molecular origin of the sawtooth behavior and the toughness of nacre. *Mater. Sci. Eng. C* **32**, 1542–1547 (2012).
5. C. E. Sing, S. L. Perry, Recent progress in the science of complex coacervation. *Soft Matter* **16**, 2885–2914 (2020).
6. S. Manoj Lalwani, C. I. Eneh, J. L. Lutkenhaus, Emerging trends in the dynamics of polyelectrolyte complexes. *Phys. Chem. Chem. Phys.* **22**, 24157–24177 (2020).
7. P. Schaaf, J. B. Schlenoff, Saloplastics: Processing compact polyelectrolyte complexes. *Adv. Mater.* **27**, 2420–2432 (2015).
8. P. Suarez-Martinez, P. Batys, M. Sammalkorpi, J. Lutkenhaus, Time–temperature and time–water superposition principles applied to poly(allylamine)/poly(acrylic acid) complexes. *Macromolecules* **52**, 3066–3074 (2019).
9. S. M. Lalwani, P. Batys, M. Sammalkorpi, J. L. Lutkenhaus, relaxation times of solid-like polyelectrolyte complexes of varying pH and water content. *Macromolecules* **54**, 7765–7776 (2021).
10. Y. Zhang, P. Batys, J. T. O'Neal, F. Li, M. Sammalkorpi, J. L. Lutkenhaus, Molecular origin of the glass transition in polyelectrolyte assemblies. *ACS Cent Sci.* **4**, 638–644 (2018).
11. Y. Zhang, F. Li, L. D. Valenzuela, M. Sammalkorpi, J. L. Lutkenhaus, Effect of water on the thermal transition observed in poly(allylamine hydrochloride)–poly(acrylic acid) complexes. *Macromolecules* **49**, 7563–7570 (2016).
12. A. S. Michaels, Polyelectrolyte complexes. *Indian J Pharm Sci.* **57**, 32–40 (1965).
13. L. Zhang, N. R. Brostowitz, K. A. Cavicchi, R. A. Weiss, Perspective: Ionomer research and applications. *Macromol. React. Eng.* **8**, 81–99 (2014).
14. S. Wu, X. Cao, Z. Zhang, Q. Chen, Y. Matsumiya, H. Watanabe, Molecular design of highly stretchable ionomers. *Macromolecules* **51**, 4735–4746 (2018).
15. C. W. Lantman, W. J. MacKnight, R. D. Lundberg, Structural properties of ionomers. *Annu. Rev. Mater.* **19**, 295–317 (1989).
16. M. Freemantle, T. Welton, R. D. Rogers, *An Introduction to Ionic Liquids* (Royal Society of Chemistry, 2019).
17. J. Yuan, M. Antonietti, Poly(ionic liquid)s: Polymers expanding classical property profiles. *Polymer* **52**, 1469–1482 (2011).
18. M. Lee, S. L. Perry, R. C. Hayward, Complex coacervation of polymerized ionic liquids in non-aqueous solvents. *ACS Polym Au.* **1**, 100–106 (2021).
19. W. Denissen, J. M. Winne, F. E. Du Prez, Vitrimers: Permanent organic networks with glass-like fluidity. *Chem. Sci.* **7**, 30–38 (2016).
20. J. van der Gucht, E. Spruijt, M. Lemmers, M. A. C. Stuart, Polyelectrolyte complexes: Bulk phases and colloidal systems. *J. Colloid Interface Sci.* **361**, 407–422 (2011).
21. J. Fu, J. B. Schlenoff, Driving forces for oppositely charged polyion association in aqueous solutions: Enthalpic, entropic, but not electrostatic. *J. Am. Chem. Soc.* **138**, 980–990 (2016).
22. Q. Wang, J. B. Schlenoff, The polyelectrolyte complex/coacervate continuum. *Macromolecules* **47**, 3108–3116 (2014).
23. J. Li, B. A. Krishna, G. van Ewijk, D. J. van Dijken, W. M. de Vos, J. van der Gucht, A comparison of complexation induced brittleness in PEI/PSS and PEI/NaPSS single-step coatings. *Colloids Surf. A Physicochem. Eng. Asp.* **648**, 129143 (2022).
24. A. W. Imre, M. Schönhoff, C. Cramer, A conductivity study and calorimetric analysis of dried poly(sodium 4-styrene sulfonate)/poly(diallyldimethylammonium chloride) polyelectrolyte complexes. *J Chem Phys.* **128**, 134905 (2008).
25. X. Lyu, B. Clark, A. M. Peterson, Thermal transitions in and structures of dried polyelectrolytes and polyelectrolyte complexes. *J Polym Sci B* **55**, 684–691 (2017).
26. R. F. Shamoun, H. H. Hariri, R. A. Ghostine, J. B. Schlenoff, Thermal transformations in extruded saloplastic polyelectrolyte complexes. *Macromolecules* **45**, 9759–9767 (2012).
27. M. B. Huglin, L. Webster, I. D. Robb, Complex formation between poly(4-vinylpyridinium chloride) and poly[sodium(2-acrylamido-2-methyl propane sulfonate)] in dilute aqueous solution. *Polymer* **37**, 1211–1215 (1996).
28. B. A. Krishna, J. D. Willott, S. Lindhoud, W. M. de Vos, Hot-pressing polyelectrolyte complexes into tunable dense saloplastics. *Polymer* **242**, 124583 (2022).
29. S. Tabandeh, L. Leon, Engineering peptide-based polyelectrolyte complexes with increased hydrophobicity. *Molecules* **24**, 868 (2019).
30. K. Sadman, Q. Wang, Y. Chen, B. Keshavarz, Z. Jiang, K. R. Shull, Influence of hydrophobicity on polyelectrolyte complexation. *Macromolecules* **50**, 9417–9426 (2017).
31. M. Yang, S. L. Sonawane, Z. A. Digby, J. G. Park, J. B. Schlenoff, Influence of "Hydrophobicity" on the composition and dynamics of polyelectrolyte complex coacervates. *Macromolecules* **55**, 7594–7604 (2022).
32. L. Xu, J. F. Ankner, S. A. Sukhishvili, Steric effects in ionic pairing and polyelectrolyte interdiffusion within multilayered films: A neutron reflectometry study. *Macromolecules* **44**, 6518–6524 (2011).
33. X. Colin, A. Tcharkhtchi, Thermal degradation of polymers during their mechanical recycling (2013).
34. R. J. Roe, J. Curro, Small-angle x-ray scattering study of density fluctuation in polystyrene annealed below the glass transition temperature. *Macromolecules* **16**, 428–434 (1983).
35. D. Montarnal, M. Capelot, F. Tournilhac, L. Leibler, Silica-like malleable materials from permanent organic networks. *Science* **334**, 965–968 (2011).
36. E. Spruijt, S. A. van den Berg, M. A. Cohen Stuart, J. van der Gucht, Direct measurement of the strength of single ionic bonds between hydrated charges. *ACS Nano* **6**, 5297–5303 (2012).
37. L. Li, S. Srivastava, S. Meng, J. M. Ting, M. V. Tirrell, Effects of non-electrostatic intermolecular interactions on the phase behavior of ph-sensitive polyelectrolyte complexes. *Macromolecules* **53**, 7835–7844 (2020).
38. T. Ameringer, F. Ercole, K. M. Tsang, B. R. Coad, X. Hou, A. Rodda, D. R. Nisbet, H. Thissen, R. A. Evans, L. Meagher, J. S. Forsythe, Surface grafting of electrospun fibers using ATRP and RAFT for the control of biointerfacial interactions. *Biointerphases* **8**, 16 (2013).
39. V. Vajihinejad, S. P. Gumfekar, D. V. Dixon, M. A. Silva, J. B. P. Soares, Enhanced dewatering of oil sands tailings by a novel water-soluble cationic polymer. *Sep. Purif. Technol.* **260**, 118183 (2021).
40. R. Meziane, J.-P. Bonnet, M. Courty, K. Djellab, M. Armand, Single-ion polymer electrolytes based on a delocalized polyanion for lithium batteries. *Electrochim. Acta* **57**, 14–19 (2011).
41. T. N. T. Phan, A. Ferrand, H. T. Ho, L. Liénafa, M. Rollet, S. Maria, R. Bouchet, D. Gigmes, Vinyl monomers bearing a sulfonyl(trifluoromethane sulfonyl) imide group: Synthesis and polymerization using nitroxide-mediated polymerization. *Polymer Chemistry* **7**, 6901–6910 (2016).
42. R. A. Ghostine, R. F. Shamoun, J. B. Schlenoff, Doping and diffusion in an extruded saloplastic polyelectrolyte complex. *Macromolecules* **46**, 4089–4094 (2013).
43. J. Fu, H. M. Fares, J. B. Schlenoff, Ion-pairing strength in polyelectrolyte complexes. *Macromolecules* **50**, 1066–1074 (2017).

44. O. Glatter, O. Kratky, *Small-Angle X-ray Scattering* (Academic Press, 1982).
45. A. B. Marciel, S. Srivastava, M. V. Tirrell, Structure and rheology of polyelectrolyte complex coacervates. *Soft Matter* **14**, 2454–2464 (2018).
46. C. G. Lopez, S. E. Rogers, R. H. Colby, P. Graham, J. T. Cabral, Structure of sodium carboxymethyl cellulose aqueous solutions: A SANS and rheology study. *J Polym Sci B* **53**, 492–501 (2015).

Acknowledgments: We acknowledge S. Pujari for performing the XPS measurements. H. van der Kooij is acknowledged for providing SEM images. We thank the Wageningen Electron Microscopy Centre (WEMC) of Wageningen University & Research for access to facilities. **Funding:** This work was supported by the Dutch Research Council (NWO) OCENW.KLEIN.326 (J.v.d.G.). **Author contributions:** Conceptualization: S.G.M.v.L., J.S., and J.v.d.G. Methodology: S.G.M.v.L., D.W.t.B., G.P., and A.P. Investigation: S.G.M.v.L., D.W.t.B., and G.P. Visualization: S.G.M.v.L. Supervision: J.S. and J.v.d.G. Writing—original draft: S.G.M.v.L., D.W.t.B., G.P., J.S., and J.v.d.G. Writing—review and editing: S.G.M.v.L., D.W.t.B., G.P., A.P., J.S., and J.v.d.G. **Competing interests:** The authors declare that they have no competing interests. **Data and materials availability:** All data needed to evaluate the conclusions in the paper are present in the paper and/or the Supplementary Materials.

Submitted 21 April 2023
Accepted 13 December 2023
Published 10 January 2024
10.1126/sciadv.adi3606

Science Advances

Moderated ionic bonding for water-free recyclable polyelectrolyte complex materials

Sophie G. M. van Lange, Diane W. te Brake, Giuseppe Portale, Anbazhagan Palanisamy, Joris Sprakel, and Jasper van der Gucht

Sci. Adv. **10** (2), eadi3606. DOI: 10.1126/sciadv.adi3606